Acta Cryst. (1992). A**48**, 247-259

Anisotropy of Anomalous Scattering in X-ray Diffraction. II. Combining Polarization-Dependent Transmission and Diffraction, and an Application to Partial-Structure Analysis

BY A. KIRFEL AND A. PETCOV

Universität des Saarlandes, FR Kristallographie, W-6600 Saarbrücken 11, Germany

(*Received* 9 *March* 1991; *accepted* 27 *September* 1991)

Abstract

The superposition of polarization-dependent X-ray transmission through crystals and resonant Bragg diffraction in crystals is investigated both theoretically and experimentally. The effects of anisotropic anomalous scattering (AAS) on the intensity of kinematically diffracted X-radiation emerging from an anisotropically absorbing crystal are described in a model that combines scattering in both forward and reverse directions. The model based on site-symmetry-compatible second-rank scattering-factor tensors for the absorbing atoms implies an additional intensity dependence on the rotation (Ψ) about the scattering vector **h**. The derived intensity function, $I(\mathbf{h}; \Psi)$, includes the usually factorized corrections for polarization and absorption. The model is applied to reflections in $LiHSeO_3$ (orthorhombic, space group $P2_12_12_1$). The systematic extinction rules for the axial reflections with odd indices can be violated by AAS. These 'forbidden' reflections are then due exclusively to the partial structure of the Se 'edge' atom, and a set of possible Se-atom positions can be derived from the relative intensity variations, $I(\mathbf{h}; \Psi)$, of only a few such 'forbidden' reflections. Experimental proof was obtained by synchrotron-radiation (using DORIS II at HASYLAB/DESY) X-ray diffraction measurements at the Se K-absorption edge ($E = 12.654$ keV) using a large synthetic $LiHSeO_3$ crystal. Significant anisotropy of anomalous scattering was observed permitting studies of both 'forbidden' ($0k0, 00l$) and allowed ($00l$) reflections. With anisotropic absorption included in the model, indications for z(Se) and y(Se) were obtained from only four 'forbidden' $00l$ and three 'forbidden' $0k0$ reflections, respectively. The experimental values are $z(\text{Se}) = 0.2375\,(125)$ and $y(\text{Se}) = 0.150\,(5)$ compared to the true values $z = 0.23316\,(4)$ and $y = 0.14709\,(2)$.

Introduction

The anisotropy of the anomalous dispersion (AAD) of X-rays is an energy-dependent resonance effect which is likely to occur in the vicinity of an absorption edge of a bonded atom. It is a consequence of chemical bonding and is reflected in two distinct phenomena in the XANES and EXAFS regions, respectively:

(i) dipole and quadrupole transitions from the initial 'core' state to allowed states which are related to the local symmetry and the chemical environment of the absorbing 'edge' atom;

(ii) interference of the outgoing wave of 'true' photoelectrons, *i.e.* with positive energy, with the wave backscattered from surrounding neighbor atoms.

In two previous contributions, Petcov, Kirfel & Fischer (1990) and Kirfel, Petcov & Eichhorn (1991), hereafter referred to as PKF and KPE, respectively, we have reported model calculations of and synchrotron radiation (SR) experiments on the effects of AAD on both X-ray transmission and kinematic X-ray diffraction. While the first paper dealt solely with dichroism and birefringence, investigated for ferroelectric lithium niobate, $LiNbO_3$, the second study was devoted to prove FRED (forbidden reflection near-edge diffraction), *i.e.* violations of extinction rules for the cases of cubic cuprite, Cu_2O, and tetragonal rutile-type TiO_2 and MnF_2, and to corroborate the predicted intensity dependencies upon rotations (Ψ) around the scattering vector. Thus, in both studies we have given analytical evaluations of the properties of the transmitted or diffracted radiation, in each case on the basis of the Jones (1941, 1948) calculus which describes the interaction of polarized electromagnetic waves with crystalline material. The resulting intensity formulae could be verified by experiment (in case of diffraction on a relative scale only). The anisotropy of the refractive index (being absent in cubic crystals) was neglected for the rutile-type crystals.

Fanchon & Hendrickson (1990) have published an investigation of the effect on the MAD (multiple-wavelength anomalous dispersion) phasing method giving a concise description of the diffraction model and reporting for the first time its use in a general least-squares program. Since the abbreviation AAS (anisotropy of anomalous scattering) used in their paper seems more appropriate than AAD and in order to use a common nomenclature in future work, we adopt it in the following.

0108-7673/92/030247-13$03.00

In the present contribution we have extended our considerations to an explicit description of the effects caused by both diffraction and transmission in case of AAS. The models developed in PKF and KPE are now combined into a more general description which allows the calculation of an integrated reflection intensity as a function of:

AAS of the 'edge' atom(s) in the structure;

intensity and polarization of the incident radiation;

size and shape of the crystal;

azimuthal setting (Ψ) of the crystal.

The resulting algorithm is rather involved and in practice requires evaluation by a computer. For special cases, however, *e.g.* restriction to serial reflections and symmetric scattering of linearly polarized radiation from an extended face of an 'infinite' crystal, it is possible to obtain tractable intensity expressions which give a detailed account of the AAS effect on the intensities of both allowed and 'forbidden' reflections, including anisotropic absorption.

For a structure crystallizing in space group $P2_12_12_1$ and with one 'edge atom' of a given element per asymmetric unit, we have recently discussed a scheme to determine a set of possible positions of that atom from the relative intensity variations $I(\mathbf{h}; \Psi)$ of a small number of 'forbidden' axial reflections (Kirfel & Petcov, 1991). This method being independent of the properties of the rest of the structure and requiring merely the occurrence of AAS, but no quantities on absolute scale, needed to be tested experimentally.

The following contribution is therefore divided into:

(i) an attempt to develop a general model for the calculation of kinematic Bragg scattering from crystals exhibiting AAS; and

(ii) an application to $LiHSeO_3$ (space group $P2_12_12_1$). This compound was chosen for two reasons. Firstly, the physical properties (dielectric, optical, piezoelectric, electro-optic, elastic and thermoelastic) exhibit considerable anisotropy (Recker, Wallrafen, Haussühl & Shao Zong Shu, 1984), implying a high probability for AAS. Secondly, the large specimen described by the above authors was available for analysis. The investigation of AAS in $LiHSeO_3$ thus includes the derivation of intensity functions from model (i) and experimental evidence of:

the occurrence of AAS at the Se K-absorption edge;

the validity and applicability of the derived model to the observations;

the possibility to extract information about the edge atom's partial structure from only a few 'forbidden' reflections.

Elastic scattering and transmission in the Jones formalism

The incident and diffracted beam together define the scattering plane which may be vertical, as depicted in Fig. 1. Directions perpendicular and parallel to that plane are denoted by indices σ and π, respectively. A totally polarized electromagnetic plane wave of incident radiation may be represented by a complex column vector of the electric field

$$|D\rangle_0 = \begin{pmatrix} A_{0\sigma} \\ A_{0\pi} \end{pmatrix}. \qquad (1)$$

Transmission through and kinematic Bragg scattering from a block inside a mosaic crystal of finite volume V_c can then be modeled in three steps (Fig. 2), each describing the action of a separate optical element.

(1) Transmissions of the incident beam along $\mathbf{t}_i = \mathbf{r} - \mathbf{r}_i$. In a material exhibiting anisotropy of the refractive index for X-ray energies, $|D\rangle_0$ will be changed to $|D\rangle_1$ by an operator $\mathfrak{M}(\mathbf{t}_i) = \mathfrak{M}_i$ describing anisotropic absorption and birefringence,

$$|D(\boldsymbol{t}_i)\rangle_1 = \mathfrak{M}_i |D\rangle_0. \qquad (2)$$

(2) Bragg diffraction under the scattering angle $2\Theta_0 \neq 0$ by the volume element dV. With the assumption that dV is so thin that there is no absorption of radiation and that the effect of interaction of the scattered and incident radiation fields can be neglected, *i.e.* there is a refractive index of unity in dV, the

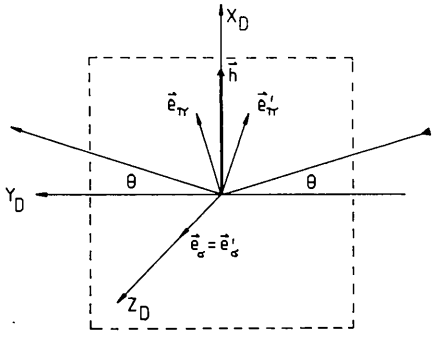

Fig. 1. Scattering geometry for the diffractometer system (D) in the reflection position. The vertical scattering plane contains $\mathbf{e}_\pi$ and $\mathbf{e}_{\pi'}$.

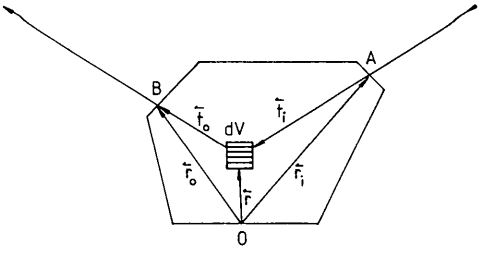

Fig. 2. Scattering-volume element dV inside the crystal. O: arbitrary origin; $\mathbf{t}_i$, $\mathbf{t}_o$: vectors describing incident and reflected beams.

scattered radiation can be written as

$$J(\varepsilon)|D(\mathbf{t}_i;\mathbf{h})\rangle_{0\Theta} = J(\varepsilon)\mathfrak{F}(\mathbf{h})|D(\mathbf{t}_i)\rangle_1. \quad (3)$$

$\mathfrak{F}(\mathbf{h})$ is the scattering operator as defined below. Following the derivation of James (1982; p. 35), $J(\varepsilon)$ is a scalar complex function which describes the superposition of waves reflected from subsequent net planes. ε is a small angular offset from Θ_0 ($\Theta = \Theta_0 + \varepsilon$).

(3) Transmission of the outgoing beam along $\mathbf{t}_o = \mathbf{r}_o - \mathbf{r}$, which modifies the diffracted radiation $|D\rangle_{0\Theta}$ into

$$J(\varepsilon)|D(\mathbf{t}_i;\mathbf{h};\mathbf{t}_o)\rangle_{1\Theta} = \mathfrak{M}_o J(\varepsilon)|D(\mathbf{t}_i;\mathbf{h})\rangle_{0\Theta}. \quad (4)$$

For the derivation of the intensity it is assumed that $\mathfrak{M}_i$ and $\mathfrak{M}_o$ are independent of small variations in Θ, *i.e.* they do not change upon rocking the crystal through the reflection position Θ_0. This approximation seems justified, since, even for a crystal rotation of one degree, the refractive index will not change appreciably with respect to the propagation directions of the incoming and outgoing waves.

Then, the integrated intensity contribution of $\mathrm{d}V$ is obtained from

$$\begin{aligned}&\mathrm{d}I(\mathbf{t}_i;\mathbf{h};\mathbf{t}_o)\\ &= {}_{\Theta 1}\langle D^*(\mathbf{t}_i;\mathbf{h};\mathbf{t}_o)|D(\mathbf{t}_i;\mathbf{h};\mathbf{t}_o)\rangle_{1\Theta} \int |J(\varepsilon)|^2 \,\mathrm{d}\varepsilon\\ &= K(\Theta)\,{}_{\Theta 1}\langle D^*(\mathbf{t}_i;\mathbf{h};\mathbf{t}_o)|D(\mathbf{t}_i;\mathbf{h};\mathbf{t}_o)\rangle_{1\Theta}\,\mathrm{d}V \quad (5a)\end{aligned}$$

where $K(\Theta)$ includes the scale factor and the Lorentz correction factor. Thus

$$\begin{aligned}&\mathrm{d}I(\mathbf{t}_i;\mathbf{h};\mathbf{t}_o)\\ &\propto {}_0\langle D^*|\mathfrak{M}_i^+\mathfrak{F}(\mathbf{h})^+\mathfrak{M}_o^+\mathfrak{M}_o\mathfrak{F}(\mathbf{h})\mathfrak{M}_i|D\rangle_0\,\mathrm{d}V \quad (5b)\end{aligned}$$

where * and $^+$ denote complex and Hermitian conjugates, respectively. Since the reflections from the different blocks of the mosaic crystal are optically independent, *i.e.* there is no regular phase relationship between them, the total observed intensity is then obtained from the summation over all contributions $\mathrm{d}I$ or from the integral:

$$I(\mathbf{h}) = K(\Theta)\int {}_{\Theta 1}\langle D^*|D\rangle_{1\Theta}\,\mathrm{d}V \quad (6)$$

taken over the crystal volume V_c.

This three-step concept includes the conventional absorption correction of a reflection intensity, extended to account explicitly for effects caused by AAS on both X-ray diffraction and transmission. This extension precludes the usual factorization of absorption and polarization corrections. The model thus represents a combination of the treatments of transmissions and kinematic Bragg diffraction as outlined in PKF and KPE, respectively.

According to (5) and (6), the calculation of $I(\mathbf{h})$ requires

(i) evaluation of $\mathrm{d}I$ and

(ii) integration over V_c.

While (ii) is a procedure which may be carried out in one step, either analytically (under favorable geometric conditions) or numerically, (i) comprises a sequence of substeps which deal with the evaluation of the:

(i*a*) refractive index of the material;

(i*b*) refractive indices experienced by the σ- and π-polarized radiation components of both the incoming and outgoing beams;

(i*c*) path lengths $|\mathbf{t}_i(\mathbf{r})|$ and $|\mathbf{t}_o(\mathbf{r})|$ for $\mathrm{d}V$ at $\mathbf{r}$;

(i*d*) operators $\mathfrak{M}_i$ and $\mathfrak{M}_o$ from (i*a*)–(i*c*);

(i*e*) structure-factor tensor $\mathbf{F}(\mathbf{h})$;

(i*f*) scattering operator $\mathfrak{F}(\mathbf{h})$;

(i*g*) complex radiation vector $|D\rangle_{1\Theta}$;

(i*h*) complex conjugated product ${}_{\Theta 1}\langle D^*|D\rangle_{1\Theta}$.

This sequence is a helpful scheme for programming. However, for the discussion of (i), it is more instructive to start with (i*g*) and (i*h*). From PKF and KPE, the operators $\mathfrak{M}$ and $\mathfrak{F}$ are given by 2×2 matrices with complex elements which, in general, depend not only on the scattering vector $\mathbf{h}$ but also on the azimuthal setting Ψ, *i.e.* a rotation of the crystal around $\mathbf{h}$. These dependencies will be discussed later. Here it suffices to define

$$\mathfrak{F}(\mathbf{h}) = \begin{pmatrix} \Phi_{\sigma'\sigma} & \Phi_{\sigma'\pi} \\ \Phi_{\pi'\sigma} & \Phi_{\pi'\pi} \end{pmatrix} \quad (7a)$$

and for a linear pleochroic and birefringent crystal

$$\mathfrak{M}_x = \begin{pmatrix} M_{x\sigma\sigma} & 0 \\ 0 & M_{x\pi\pi} \end{pmatrix} \qquad (x = i, o). \quad (7b)$$

The description of the scattering operator $\mathfrak{F}$, its elements Φ and absorption-free scattering was the subject of KPE which includes a detailed account of the practical evaluation of reflection intensities obtained by single-crystal diffractometry.

For a discussion of scattering [items (i*e*) and (i*f*)], the reader is therefore referred to the KPE paper. Given $\mathfrak{M}_x$ and $\mathfrak{F}$, it follows that

$$\begin{aligned}|D\rangle_{1\Theta} &= \mathfrak{M}_o\mathfrak{F}\mathfrak{M}_i|D\rangle_0\\ &= \begin{pmatrix} M_{o\sigma\sigma}M_{i\sigma\sigma}\Phi_{\sigma'\sigma}A_{0\sigma} + M_{o\sigma\sigma}M_{i\pi\pi}\Phi_{\sigma'\pi}A_{0\pi} \\ M_{o\pi\pi}M_{i\sigma\sigma}\Phi_{\pi'\sigma}A_{o\sigma} + M_{o\pi\pi}M_{i\pi\pi}\Phi_{\pi'\pi}A_{0\pi} \end{pmatrix}\end{aligned} \quad (8)$$

and

$$\begin{aligned}{}_{\Theta 1}\langle D^*|D\rangle_{1\Theta} &= |A_{o\sigma}|^2|M_{i\sigma\sigma}|^2(|M_{o\sigma\sigma}|^2|\Phi_{\sigma'\sigma}|^2\\ &\quad + |M_{o\pi\pi}|^2|\Phi_{\pi'\sigma}|^2)\\ &\quad + |A_{o\pi}|^2|M_{i\pi\pi}|^2(|M_{o\sigma\sigma}|^2|\Phi_{\sigma'\pi}|^2\\ &\quad + |M_{o\pi\pi}|^2|\Phi_{\pi'\pi}|^2) + 2\,\mathrm{Re}\,(A_{o\sigma}^* A_{o\pi}\Sigma)\end{aligned} \quad (9)$$

with

$$\begin{aligned}\Sigma &= |M_{o\sigma\sigma}|^2 M_{i\sigma\sigma}^*\Phi_{\sigma'\sigma}^* M_{i\pi\pi}\Phi_{\sigma'\pi}\\ &\quad + |M_{o\pi\pi}|^2 M_{i\sigma\sigma}^*\Phi_{\pi'\sigma}^* M_{i\pi\pi}\Phi_{\pi'\pi}.\end{aligned} \quad (10)$$

Equation (9) simplifies considerably and depends only on the moduli of the complex elements of the $\mathfrak{F}$ and $\mathfrak{M}$ operator if

(*a*) the incident radiation is purely σ or π polarized ($A_{0\pi}=0$ or $A_{0\sigma}=0$, respectively) or

(*b*) $\Sigma=0$ owing to either $\Phi_{\sigma'\sigma}=\Phi_{\pi'\pi}=0$ or $\Phi_{\pi'\sigma}=\Phi_{\sigma'\pi}=0$ (see KPE).

For unpolarized radiation, a scalar structure factor $F(\mathbf{h})(\Phi_{\pi'\sigma}=\Phi_{\sigma'\pi}=0)$ and an isotropic refractive index ($M_{i\sigma\sigma}=M_{i\pi\pi}$), (9) reduces to

$$\mathrm{d}I(\mathbf{h})\propto|M_{i\sigma\sigma}|^2|M_{o\sigma\sigma}|^2(1+\cos^2 2\Theta)|F(\mathbf{h})|^2. \quad (11)$$

$(1+\cos^2 2\Theta)$ is the Thomson polarization-correction factor and

$$|M_{i\sigma\sigma}|^2|M_{o\sigma\sigma}|^2=\exp\{-\mu[|\mathbf{t}_i(\mathbf{h};\mathbf{r})|+|\mathbf{t}_o(\mathbf{h};\mathbf{r})|]\} \quad (12)$$

corrects for the isotropic absorption. Thus, in (9) the $|M|^2$ factors describe merely the anisotropic attenuation, whereas Σ accounts also for photon–crystal interactions involving a defined phase relation between the σ- and π-polarized components of the radiation. A reflection intensity can therefore be affected by X-ray birefringence as soon as the incident radiation is not totally σ or π polarized *and* $\Sigma\neq 0$ [(*a*) and (*b*) not obeyed].

For an intensity contribution dI, the influence of birefringence is confined to the incoming radiation, *i.e.* different volume elements receive radiation of different properties. After scattering, the diffracted radiation will also, of course, be modified by birefringence, although only with respect to its polarization in agreement with equation (13) of PKF.

Synchrotron radiation (SR) is often considered as totally σ polarized. More precisely, it is elliptically polarized with the major axis of the section parallel to σ;

$$|D\rangle_0=A_0\begin{pmatrix}1\\ ip\end{pmatrix}$$

where $|p|\leq 1$ is related to the degree of the linear horizontal polarization $L_\sigma=(1-p^2)/(1+p^2)$. $|p|$ is typically about 0.2. Neglecting the second term of (9) containing p^2, one obtains

$$\begin{aligned}
&{}_\Theta\langle D^*|D\rangle_\Theta\\
&\simeq A_0^2[|M_{i\sigma\sigma}|^2(|M_{o\sigma\sigma}|^2|\Phi_{\sigma'\sigma}|^2\\
&\quad+|M_{o\pi\pi}|^2|\Phi_{\pi'\sigma}|^2)+2p\ \mathrm{Re}\,(i\Sigma)]\\
&\simeq A_0^2|M_{i\sigma\sigma}|^2[|M_{o\sigma\sigma}|^2|\Phi_{\sigma'\sigma}|^2+|M_{o\pi\pi}|^2|\Phi_{\pi'\sigma}|^2]\\
&\quad-2pA_0^2|M_{i\sigma\sigma}|^2\{|M_{o\sigma\sigma}|^2[a\ \mathrm{Im}\,(\Phi^*_{\sigma'\sigma}\Phi_{\sigma'\pi})\\
&\quad+b\ \mathrm{Re}\,(\Phi_{\sigma'\sigma}\Phi_{\sigma'\pi})]+|M_{o\pi\pi}|^2[a\ \mathrm{Im}\,(\Phi^*_{\pi'\sigma}\Phi_{\pi'\pi})\\
&\quad+b\ \mathrm{Re}\,(\Phi_{\pi'\sigma}\Phi_{\pi'\pi})]\} \qquad (13)
\end{aligned}$$

with $a=\mathrm{Re}\,(M^*_{i\sigma\sigma}M_{i\pi\pi})$ and $b=\mathrm{Im}\,(M^*_{i\sigma\sigma}M_{i\pi\pi})$. For $p=0$, (13) yields the effect of pure σ polarization.

Refractive index and X-ray transmission

Using atomic scattering-factor tensors **f** and the structure-factor tensor **F**(**h**) as outlined in KPE, an anisotropic refractive index, **n**, can be written in a Cartesian system as (James, 1982)

$$\begin{aligned}
\mathbf{n}&=\mathbf{I}-\kappa(\mathbf{B}_0^{-1})^T\mathbf{F}(0)(\mathbf{B}_0^{-1})\\
&=\mathbf{I}[1-\kappa F(0)_0]-\kappa(\mathbf{B}_0^{-1})^T\mathbf{F}(0)_a(\mathbf{B}_0^{-1}) \qquad (14)
\end{aligned}$$

with

$$\kappa=\lambda^2 e^2/2\pi m_e c^2 V_o,$$

where $e^2/m_e c^2$ is the electron radius and V_o is the unit-cell volume.

$\mathbf{B}_0^T$ describes the unit vectors of the reciprocal lattice with respect to a Cartesian system (C) in the crystal where $\mathbf{X}_C\parallel\mathbf{a}_o^*$, $\mathbf{Y}_C\parallel\mathbf{a}_o^*\times\mathbf{c}_o$ and $\mathbf{Z}_C\parallel\mathbf{a}_o^*\times\mathbf{b}_o^*$. $\mathbf{B}_0\mathbf{B}_0^T=\mathbf{G}_0^*$ can be obtained from the reciprocal metric tensor for $a^*=b^*=c^*=1$ ($\mathbf{B}_0$ and $\mathbf{G}_0^*$ are equal to **I** for orthogonal crystal axes, **I** is the matrix of unity).

$$\begin{aligned}
F(0)_0&=\sum_j^n\sum_k^m c_j(Z_j+if''_{0j})\\
&=m\sum_j^n c_j(Z_j+f'_{0j}+if''_{0j}) \qquad (15)\\
\mathbf{F}(0)_a&=\sum_j^n\sum_k^m c_j[(\mathbf{f}'_{jk}-\mathbf{G}_0^*f'_{0j})+i(\mathbf{f}''_{jk}-\mathbf{G}_0^*\mathbf{f}''_{0j})]
\end{aligned}$$

where n is the number of atoms in the asymmetric unit, m is the number of symmetry operations of the space group, c_j is the multiplicity (occupation factor), Z is the atomic number and f'_0 and f''_0 are the isotropic anomalous dispersion correction factors.

Since $\mathbf{f}_{jk}$ is the complex scattering-factor tensor of the jth atom transformed by the rotational part of the kth symmetry operation,

$$\mathbf{f}_{jk}=\mathbf{R}_k\mathbf{f}_{j1}\mathbf{R}_k^T. \qquad (16)$$

n is described by a tensor which is invariant against all point-symmetry operations and $\mathbf{F}(0)_a$ determines the anisotropy of the refractive index.

The index experienced by a σ-polarized wave is found from the intersection of the projection of **n** onto the plane perpendicular to the propagation direction with the σ direction

$$n_\sigma=\mathbf{e}_\sigma^T\mathbf{n}\mathbf{e}_\sigma \qquad (17)$$

where $\mathbf{e}_\sigma$ is the unit vector of the polarization direction. The real part n_σ of n_σ and the corresponding absorption coefficient μ_σ (from the optical theorem) are then, with $\xi=\lambda/4\pi$,

$$\begin{aligned}
n_\sigma&=1-\kappa\ \mathrm{Re}\,[F(0)_0+\Phi_{a\sigma\sigma}(0)]\\
\mu_\sigma&=(\kappa/\xi)\ \mathrm{Im}\,[F(0)_0+\Phi_{a\sigma\sigma}(0)] \qquad (18)
\end{aligned}$$

with

$$\Phi_{a\sigma\sigma}(0)=\mathbf{e}_\sigma^T(\mathbf{B}_0^{-1})^T\mathbf{F}(0)_a(\mathbf{B}_0^{-1})\mathbf{e}_\sigma. \qquad (19)$$

Using $\mathbf{e}_\pi$ for the incident and $\mathbf{e}_{\pi'}$ for the outgoing beam (see Fig. 1) in the same way yields similarly n_π, μ_π and $n_{\pi'}$, $\mu_{\pi'}$ from $\Phi_{a\pi\pi}(0)$ and $\Phi_{a\pi'\pi'}(0)$, respecitvely. The complex numbers Φ thus correspond to the elements of $\mathfrak{F}$ [equation (8) of KPE], calculated, however, for $\mathbf{h}=0$ and combinations of identical $\mathbf{e}$.

According to equation (9) of PKF, the elements of the operators $\mathfrak{M}_i$ and $\mathfrak{M}_o$ are then given by ($t_i=|\mathbf{t}_i|$)

$$\begin{aligned} M_{i\eta\eta} &= \exp\{-[i(\omega/c)n_{\eta\eta}+\mu_{\eta\eta}/2]t_i\} \\ &\qquad (\eta\eta=\sigma\sigma \text{ or } \pi\pi) \\ M_{o\nu\nu} &= \exp\{-[i(\omega/c)n_{\nu\nu}+\mu_{\nu\nu}/2]t_o\} \\ &\qquad (\nu\nu=\sigma\sigma \text{ or } \pi'\pi') \end{aligned} \tag{20}$$

so that, with $\eta=\sigma$ or π and $\nu=\sigma$ or π',

$$\begin{aligned} \text{and} \qquad |M_{i\eta\eta}|^2 &= \exp[-\mu_{\eta\eta}t_i] \\ |M_{o\nu\nu}|^2 &= \exp[-\mu_{\nu\nu}t_o]. \end{aligned} \tag{21}$$

Setting $\mu=(\mu_{\sigma\sigma}+\mu_{\pi\pi})/2$ and $\Delta\mu=\mu_{\sigma\sigma}-\mu_{\pi\pi}$, one obtains for the coefficients a and b of (13):

$$\begin{aligned} a &= \cos[(\omega/c)\Delta\mu t_i]\exp[-\mu t_i] \\ b &= \sin[(\omega/c)\Delta\mu t_i], \end{aligned} \tag{22}$$

showing that, for a given crystal orientation, the intensity contributions from the volume elements $\mathrm{d}V$ can be modulated by birefringence (*i.e.* through oscillating functions of the pathlengths t_i).

Now one has to recall that the unit vectors of the polarization directions, $\mathbf{e}_\sigma$, $\mathbf{e}_\pi$ and $\mathbf{e}_{\pi'}$, all taken with respect to the crystal, depend on $\mathbf{h}$ and the azimuth Ψ. Thus, the $n_{\eta\eta}$ and $\mu_{\eta\eta}$ values are actually $n_{\eta\eta}(\mathbf{h};\Psi)$ and $\mu_{\eta\eta}(\mathbf{h};\Psi)$, $\eta=\sigma$, π, π', and must be evaluated from $\mathbf{n}$ [see (18)] for every combination $(\mathbf{h};\Psi)$. For bisecting geometry, the calculations required for the transformation of a structure-factor tensor into the diffractometer system (D) have been described in detail in KPE. With the same arguments and notation, it is seen that the complex numbers $\Phi_{a\eta\eta}$ of (18) are given by equation (28) of KPE, slightly modified to

$$\begin{aligned} \Phi_{a\eta\eta}(\mathbf{h};\Psi) &= \mathbf{e}_{\eta D}^T(\boldsymbol{\Psi}\mathbf{X}_0\boldsymbol{\Phi}_0)(\mathbf{B}_0^{-1})^T\mathbf{F}(0)_a \\ &\quad\times(\mathbf{B}_0^{-1})(\boldsymbol{\Psi}\mathbf{X}_0\boldsymbol{\Phi}_0)^T\mathbf{e}_{\eta D}. \end{aligned} \tag{23}$$

$\mathbf{X}_0(\mathbf{h})$ and $\boldsymbol{\Phi}_0(\mathbf{h})$ are the matrices for rotations χ and φ, respectively; $\boldsymbol{\Psi}$ accounts for a Ψ rotation. From Fig. 1 follows

$$\mathbf{e}_{\sigma D}=\begin{pmatrix}0\\0\\1\end{pmatrix}, \qquad \mathbf{e}_{\pi D}=\begin{pmatrix}\cos\Theta\\\sin\Theta\\0\end{pmatrix}, \qquad \mathbf{e}_{\pi' D}=\begin{pmatrix}\cos\Theta\\-\sin\Theta\\0\end{pmatrix}. \tag{24}$$

The evaluation of (9) or (13) for a $(\mathbf{h};\Psi)$ combination is now straightforward. Equation (23) yields both the elements $\Phi_{\eta'\nu}(\mathbf{h};\Psi)$ using $\mathbf{F}(\mathbf{h})$ and the elements $\Phi_{a\eta\eta}(\mathbf{h};\Psi)$ of (18) using $\mathbf{F}(0)_a$. Insertion of the latter numbers into (18) then allows the calculation of (20)–(22) *etc.*

Application to $LiHSeO_3$

(a) The structure-factor tensor $\mathbf{F}(\mathbf{h})$ *in the diffractometer system*

The general position of Se in $LiHSeO_3$, space group $P2_12_12_1$, $Z=4$, allows the complex tensor of AAS to be general:

$$\mathbf{f}_{\mathrm{Se}}=\mathbf{f}'_{\mathrm{Se}}+i\mathbf{f}''_{\mathrm{Se}}$$

with elements

$$f_{\mathrm{Se},ij}=(f'_{\mathrm{Se},ij}-f'_{0,\mathrm{Se}}\delta_{ij})+i(f''_{\mathrm{Se},ij}-f''_{0,\mathrm{Se}}\delta_{ij}). \tag{25}$$

$f'_{0,\mathrm{Se}}$, $f''_{0,\mathrm{Se}}$ are the isotropic (free atom) real and imaginary AS correction terms and δ_{ij} is the Kronecker symbol.

With any AAS of Li, H and O neglected, the application of equation (15) of KPE and (16) yields

$$\begin{aligned} \mathbf{F}(\mathbf{h}) &= \mathbf{I}F(\mathbf{h})_0+\sum_k^4 \mathbf{R}_k[\mathbf{f}'_{\mathrm{Se}}+i\mathbf{f}''_{\mathrm{Se}}] \\ &\quad\times\mathbf{R}_k^T T(\mathbf{h})_{k,\mathrm{Se}}G(\mathbf{h})_{k,\mathrm{Se}}. \end{aligned} \tag{26}$$

Omission of the subscript Se in the following means that reflections $00l$ are therefore described by

$$\begin{aligned} \mathbf{F}(00l) &= \mathbf{I}F(00l)_0+T_{\mathrm{Se}}(00l) \\ &\quad\times\{(\mathbf{f}_1+\mathbf{f}_2\exp[\pi il])\exp[2\pi ilz] \\ &\quad+(\mathbf{f}_3+\mathbf{f}_4\exp[\pi il])\exp[-2\pi ilz]\}. \end{aligned} \tag{27}$$

With $\exp[\pi il]=(-1)^l$, $C_{lz}=\cos 2\pi lz$, $S_{lz}=\sin 2\pi lz$, and including the common temperature factor $T_{\mathrm{Se}}(00l)=\exp[-2\pi^2l^2c^{*2}u_{33}]$ into $\mathbf{f}$, (27) reduces to

$$\begin{aligned} \mathbf{F}(00l) &= \mathbf{I}F(00l)_0+C_{lz}[(\mathbf{f}_1+\mathbf{f}_3)+(-1)^l(\mathbf{f}_2+\mathbf{f}_4)] \\ &\quad+iS_{lz}[(\mathbf{f}_1-\mathbf{f}_3)+(-1)^l(\mathbf{f}_2-\mathbf{f}_4)]. \end{aligned} \tag{28}$$

Application of the rotational matrices of the symmetry operations in $P2_12_12_1$ yields the tensors $\mathbf{f}_2$ to $\mathbf{f}_4$ from $\mathbf{f}_1$, and one obtains for allowed reflections $00l$, $l=2n$,

$$\mathbf{F}(00l)=\mathbf{I}F(00l)_0+4\begin{pmatrix} f_{11}C_{lz} & if_{12}S_{lz} & 0 \\ if_{21}S_{lz} & f_{22}C_{lz} & 0 \\ 0 & 0 & f_{33}C_{lz}\end{pmatrix} \tag{29}$$

and for the 'forbidden' (systematically extinct) reflections $00l$, $l=2n+1$,

$$\mathbf{F}(00l)=4\begin{pmatrix} 0 & 0 & if_{13}S_{lz} \\ 0 & 0 & f_{23}C_{lz} \\ if_{31}S_{lz} & f_{32}C_{lz} & 0\end{pmatrix} \tag{30}$$

where f_{ij} are the complex numbers as defined in (24).

Corresponding expressions are found for the serial reflections $h00$ and $0k0$. They all yield for $\mathbf{h}=0$

$$\mathbf{F}(0)=\mathbf{I}F(0)_0+4\begin{pmatrix} f_{11} & 0 & 0 \\ 0 & f_{22} & 0 \\ 0 & 0 & f_{33}\end{pmatrix}. \tag{31}$$

From (18) and (23) follow the principal values of the refractive index for $\Theta=0°$. With the indices $i=1,2,3$ corresponding to the directions parallel to the crystallographic axes, **a**, **b**, **c**, real and imaginary parts are given by

$$\begin{aligned} n_i &= 1-\kappa\ \mathrm{Re}\,[F(0)_0+4f_{ii}] \\ \mu_i &= (\kappa/\xi)\ \mathrm{Im}\,[F(0)_0+4f_{ii}]. \end{aligned} \tag{32}$$

To obtain the structure-factor tensors $\mathbf{F}(\mathbf{h})_D$ and $\mathbf{F}(0;\mathbf{h})_D$ in the diffractometer system D (see KPE), the $\mathbf{F}(\mathbf{h})$ have to be transformed according to (23). $\mathbf{F}(0;\mathbf{h})_D$ is the structure-factor tensor for scattering in the forward direction when the crystal is in reflecting position **h**. For these calculations we assume the crystal to be mounted on the diffractometer so that $\mathbf{UB}=\mathbf{B}$. Then $\mathbf{\Phi}_0(h00)=\mathbf{X}_0(h00)=\mathbf{I}$ and $\mathbf{\Phi}_0(00l)=\mathbf{I}$, while $\mathbf{X}_0(00l)$ is determined by $\kappa=90°$. By inclusion of the Ψ rotation around the scattering vector, the $\mathbf{F}(\mathbf{h};\Psi)_D$ tensors are (after rotation of the crystal into the reflecting position):

(i) '*forbidden*' $00l$, $l=2n+1$:

$$\mathbf{F}(00l;\Psi)_D = 4\begin{pmatrix} 0 & -if_{31}S_{lz}\sin\Psi + f_{32}C_{lz}\cos\Psi & -if_{31}S_{lz}\cos\Psi - f_{32}C_{lz}\sin\Psi \\ -if_{13}S_{lz}\sin\Psi + f_{23}C_{lz}\cos\Psi & 0 & 0 \\ -if_{13}S_{lz}\cos\Psi - f_{23}C_{lz}\sin\Psi & 0 & 0 \end{pmatrix}; \tag{33}$$

(ii) *allowed* $00l$, $l=2n$:

$$\mathbf{F}(00l;\Psi)_D=\mathbf{I}F(00l)_0+4\mathbf{F}_a \tag{34}$$

with

$$\begin{aligned} F_{a11} &= f_{33}C_{lz} \\ F_{a12} &= F_{a21}=F_{a13}=F_{a31}=0 \\ F_{a22} &= C_{lz}(f_{11}\sin^2\Psi+f_{22}\cos^2\Psi) \\ &\quad -iS_{lz}(f_{12}+f_{21})\sin\Psi\cos\Psi \\ F_{a23} &= C_{lz}(f_{11}-f_{22})\sin\Psi\cos\Psi \\ &\quad +iS_{lz}(f_{12}\sin^2\Psi-f_{21}\cos^2\Psi) \\ F_{a32} &= C_{lz}(f_{11}-f_{22})\sin\Psi\cos\Psi \\ &\quad +iS_{lz}(f_{21}\sin^2\Psi-f_{12}\cos^2\Psi) \\ F_{a33} &= C_{lz}(f_{11}\cos^2\Psi+f_{22}\sin^2\Psi) \\ &\quad +iS_{lz}(f_{12}+f_{21})\sin\Psi\cos\Psi \end{aligned}$$

which reduces for the $\mathbf{F}(0;00l;\Psi)_D$ tensor to

$$\mathbf{F}(0;00l;\Psi)_D = \mathbf{I}F(0)_0+4\begin{pmatrix} f_{33} & 0 & 0 \\ 0 & f_{11}\sin^2\Psi+f_{22}\cos^2\Psi & (f_{11}-f_{22})\sin\Psi\cos\Psi \\ 0 & (f_{11}-f_{22})\sin\Psi\cos\Psi & f_{11}\cos^2\Psi+f_{22}\sin^2\Psi \end{pmatrix}. \tag{35}$$

(*b*) *The elements Φ of the operators $\mathfrak{M}$, $\mathfrak{F}$*

Equations (30) to (34) allow the calculation of the elements Φ of the operators $\mathfrak{M}_i$, $\mathfrak{M}_o$ and $\mathfrak{F}$.

(i) '*Forbidden*' $00l$

$$\begin{aligned} \Phi_{a\sigma'\sigma}(00l;\Psi) &= 0 \\ \Phi_{a\pi'\pi}(00l;\Psi) &= 2\sin 2\Theta_l[-iS_{lz}(f_{31}-f_{13})\sin\Psi \\ &\quad +C_{lz}(f_{32}-f_{23})\cos\Psi] \\ \Phi_{a\pi'\sigma}(00l;\Psi) &= -4\cos\Theta_l[if_{31}S_{lz}\cos\Psi \\ &\quad +f_{32}C_{lz}\sin\Psi] \\ \Phi_{a\sigma'\pi}(00l;\Psi) &= -4\cos\Theta_l[if_{13}S_{lz}\cos\Psi \\ &\quad +f_{23}C_{lz}\sin\Psi]. \end{aligned} \tag{36}$$

For a symmetric AAS tensor $\mathbf{f}_{\mathrm{Se}}$, $\Phi_{a\pi'\pi}=0$ and $\Phi_{a\pi'\sigma}=\Phi_{a\sigma'\pi}$. The polarization of the scattered radiation is then always orthogonal to that of the incident radiation. Thus, σ-polarized radiation will become π polarized after scattering and *vice versa*.

(ii) *Allowed* $00l$

$$\begin{aligned} \Phi_{a\sigma'\sigma}(00l;\Psi) &= 4[C_{lz}(f_{11}\cos^2\Psi+f_{22}\sin^2\Psi) \\ &\quad +iS_{lz}(f_{12}+f_{21})\sin\Psi\cos\Psi] \\ \Phi_{a\pi'\pi}(00l;\Psi) &= 4\{f_{33}C_{lz}\cos^2\Theta_l \\ &\quad -[C_{lz}(f_{11}\sin^2\Psi+f_{22}\cos^2\Psi) \\ &\quad -iS_{lz}(f_{12}+f_{21}) \\ &\quad \times\sin\Psi\cos\Psi]\sin^2\Theta_l\} \\ \Phi_{a\pi'\sigma}(00l;\Psi) &= -4\sin\Theta_l[C_{lz}(f_{11}-f_{22})\sin\Psi\cos\Psi \\ &\quad +iS_{lz}(f_{12}\sin^2\Psi-f_{21}\cos^2\Psi)] \\ \Phi_{a\sigma'\pi}(00l;\Psi) &= 4\sin\Theta_l[C_{lz}(f_{11}-f_{22})\sin\Psi\cos\Psi \\ &\quad +iS_{lz}(f_{21}\sin^2\Psi-f_{12}\cos^2\Psi)]. \end{aligned} \tag{37}$$

(iii) Consequently, one obtains for the $\mathbf{F}(0;00l;\Psi)$ tensor

$$\begin{aligned} \Phi_{a\sigma\sigma}(00l;\Psi) &= \Phi_{a\sigma'\sigma'}(00l;\Psi)=4a \\ \Phi_{a\pi\pi}(00l;\Psi) &= \Phi_{a\pi'\pi'}(00l;\Psi)=4b \end{aligned}$$

with

$$a = f_{11}\cos^2\Psi + f_{22}\sin^2\Psi$$
$$b = f_{33}\cos^2\Theta_l + (f_{11}\sin^2\Psi + f_{22}\cos^2\Psi)\sin^2\Theta_l \quad (38)$$

and, from (18),

$$\begin{aligned} n_{\sigma\sigma}(00l;\Psi) &= n_{\sigma'\sigma'} = 1-\kappa\,\mathrm{Re}\,[F(0)_0+4a] \\ n_{\pi\pi}(00l;\Psi) &= n_{\pi'\pi'} = 1-\kappa\,\mathrm{Re}\,[F(0)_0+4b] \\ \mu_{\sigma\sigma}(00l;\Psi) &= \mu_{\sigma'\sigma'} = (\kappa/\xi)\,\mathrm{Im}\,[F(0)_0+4a] \\ \mu_{\pi\pi}(00l;\Psi) &= \mu_{\pi'\pi'} = (\kappa/\xi)\,\mathrm{Im}\,[F(0)_0+4b] \end{aligned} \quad (39)$$

which can be rewritten in terms of the principal values (32) as

$$\begin{aligned} \alpha_{\sigma\sigma}(00l;\Psi) &= \alpha_{\sigma'\sigma'} \\ &= \alpha_1\cos^2\Psi + \alpha_2\sin^2\Psi \\ \alpha_{\pi\pi}(00l;\Psi) &= \alpha_{\pi'\pi'} \\ &= (\alpha_1\sin^2\Psi + \alpha_2\cos^2\Psi)\sin^2\Theta_l + \alpha_3\cos^2\Theta_l \end{aligned} \quad (40)$$

where α stands for either n or μ.

Intensities of 00*l* reflections

The following discussion is confined to a symmetric tensor $\mathbf{f}_{Se}$ and to totally σ-polarized incident radiation being regarded as a good approximation for synchrotron radiation. Generalization is straightforward, but leads to very large expressions that are not useful in the present study.

Neglecting the scale factor, one finds from (5), (13) and (19) for the scattering from a volume element dV:

$$\begin{aligned} dI(t_i;00l;t_o) &\propto |M_{i\sigma\sigma}|^2[|M_{o\sigma\sigma}|^2|\Phi_{\sigma'\sigma}|^2 \\ &\quad + |M_{o\pi'\pi'}|^2|\Phi_{\pi'\sigma}|^2]\,dV \\ &\propto \{\exp[-\mu_{\sigma\sigma}(t_i+t_o)]|\Phi_{\sigma'\sigma}|^2 \\ &\quad + \exp[-\mu_{\sigma\sigma}t_i - \mu_{\pi'\pi'}t_o]|\Phi_{\pi'\sigma}|^2\}\,dV. \end{aligned} \quad (41)$$

Considering a crystal of infinite thickness, cut parallel to (001) (Fig. 3), $t_i = t_o = y/\sin\Theta_l$ where y is the distance of the volume element dV from the surface. Since $dV = F\,dy$ and $F = d^2/\sin\Theta_l$, where d^2 gives the cross section of the beam,

$$\begin{aligned} dI(y,00l) &\propto \{\exp[-(2\mu_{\sigma\sigma}/\sin\Theta_l)y]|\Phi_{\sigma'\sigma}|^2 \\ &\quad + \exp[-(\mu_{\sigma\sigma}+\mu_{\pi\pi})y/\sin\Theta_l]|\Phi_{\pi'\sigma}|^2\} \\ &\quad \times(d^2/\sin\Theta_l)\,dy. \end{aligned} \quad (42)$$

Integration yields then for fixed d and all 00l

$$I(00l) \propto (|\Phi_{\sigma'\sigma}|^2/2\mu_{\sigma\sigma}) + [|\Phi_{\pi'\sigma}|^2/(\mu_{\sigma\sigma}+\mu_{\pi\pi})] \quad (43)$$

where all contributions are of course Ψ-dependent.

Compared to neglecting the anisotropy of absorption, *i.e.* using a mean coefficient μ, the relative intensity difference is given by

$$\begin{aligned} \Delta I/I = [&|\Phi_{\sigma'\sigma}|^2(\mu_{\sigma\sigma}+\mu_{\pi\pi})(\mu-\mu_{\sigma\sigma}) \\ &+ |\Phi_{\pi'\sigma}|^2\mu_{\sigma\sigma}(2\mu-\mu_{\sigma\sigma}-\mu_{\pi\pi})] \\ &\times[\mu_{\sigma\sigma}(\mu_{\sigma\sigma}+\mu_{\pi\pi})(|\Phi_{\sigma'\sigma}|^2+|\Phi_{\pi'\sigma}|^2)]^{-1}. \end{aligned} \quad (44)$$

(i) '*Forbidden*' *reflections* 00*l*

From (36), (40) and (43) one obtains

$$\begin{aligned} I(00l;\Psi) = \{&K_l\cos^2\Theta_l[A\sin^2\Psi \\ &+ B\cos^2\Psi + C\sin 2\Psi]\} \\ &\times[\mu_1+\mu_3+(\mu_2-\mu_3)\sin^2\Theta_l \\ &+ (\mu_2-\mu_1)\cos^2\Theta_l\sin^2\Psi]^{-1} \end{aligned} \quad (45)$$

with

$$A = |f_{23}|^2C_{lz}^2; \qquad B = |f_{13}|^2S_{lz}^2;$$
$$C = (f'_{13}f''_{23} - f'_{23}f''_{13})C_{lz}S_{lz}.$$

K_l is a scalar factor and the μ_i are given by (32). Thus, only off-diagonal elements of $\mathbf{f}_{Se}$ contribute to the reflection intensity which receives an additional modulation through a difference between μ_1 and μ_2. Equation (45) is periodic in π with extrema at $\Psi = 0$ and $\pi/2$ if only C is negligible. Otherwise, the maxima and minima will be shifted to intermediate Ψ settings.

Clearly, the numerator of (45) depends on the z coordinates of the Se atom, and the intensity ratio

$$\begin{aligned} Q(l) &= I(00l;0)/I(00l;\pi/2) \\ &= \tan^2(2\pi lz)\{|f_{13}|^2[\mu_2+\mu_3+(\mu_1-\mu_3)\sin^2\Theta_l]\} \\ &\quad \times\{|f_{23}|^2[\mu_2+\mu_1+(\mu_2-\mu_3)\sin^2\Theta_l]\}^{-1} \end{aligned} \quad (46)$$

contains phase information. The use of this information to determine the z coordinate has been proposed and discussed in detail by Kirfel & Petcov (1991), however, without consideration of anisotropic absorption. The method is based on the ratio of any two 'forbidden' reflections, $Q_{zij} = Q(l_i)/Q(l_j)$ which cancels the *a priori* unknown AAS and leaves

$$Q_{zij} = [\tan^2(2\pi l_i z)/\tan^2(2\pi l_j z)]\,Y_{zij}. \quad (47)$$

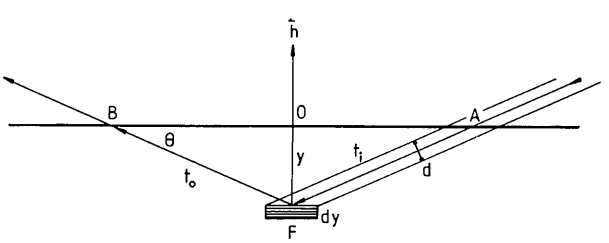

Fig. 3. Scattering-volume element $dV = F\,dy$ at depth y below the surface (AOB) of an infinite crystal. The beam cross section is d^2.

Y_{zij} contains the anisotropy of absorption and depends also on the scattering angles. With $Y=1$ (*i.e.* assuming isotropic absorption), it can be shown that the consideration of only a few Q_{zij} yields a common indication for z ($0<z\leq 0.25$), even if the quotients are associated with large experimental errors. The systematic error introduced by using $Y=1$ in (47) can be estimated from (46),

$$(\Delta Y/Y)=(a-b)(\sin^2{}_i\Theta-\sin^2{}_j\Theta)\times[(1+a\sin^2\Theta_j)(1+b\sin^2\Theta_i)]^{-1} \quad (48)$$

with $a=(\mu_1-\mu_3)/(\mu_2+\mu_3)$ and $b=(\mu_2-\mu_3)/(\mu_2+\mu_1)$.

Obviously, this error increases with increasing anisotropy in μ and/or increasing difference $\Theta_i-\Theta_j$, and should be corrected for if the $\mu_{1,2,3}$ values are known from absorption measurements. However, neglecting Y is not likely to compromise the method. Insertion into (48), for example, of rather unfavorable values such as $\mu_1:\mu_2:\mu_3=1.3:0.6:1.0$, $\Theta_i=10°$ and $\Theta_j=45°$ yields only $|\Delta Y/Y|=0.17$ which in view of an error discussion (Kirfel & Petcov, 1991) can be accommodated. Thus, model values $I(00l;0)$ and $I(00l;\pi/2)$ should be obtained from fits of the full expression (45) (rather than its numerator) to observed $I(00l;\Psi)$ curves, but assuming then isotropic μ in (47) will not give any consequences.

(ii) *Allowed reflections* $00l$

Writing the structure factor $F(00l)_0$ (which includes isotropic AS; compare KPE) as FA_0+iFB_0, one obtains from (43)

$$I(00l;\Psi)\propto[|F_0|^2+2FA_0\,\mathrm{Re}\,(\Phi_{a\sigma'\sigma})+2FB_0\,\mathrm{Im}\,(\Phi_{a\sigma'\sigma})+|\Phi_{a\sigma'\sigma}|^2]/2\mu_{\sigma\sigma}+|\Phi_{a\pi'\sigma}|^2/(\mu_{\sigma\sigma}+\mu_{\pi\pi}) \quad (49)$$

where $\Phi_{a\sigma'\sigma}$ and $\Phi_{a\pi'\sigma}$ are given by (37). Equation (49) shows that the numerical evaluation bears no difficulty, but the full analytical representation becomes rather lengthy.

It is instructive to consider (49) for two distinct cases. The first case assumes that $|F(00l)_0|$ is much greater than $|\Phi_{a\sigma'\sigma}|$ and $|\Phi_{a\pi'\sigma}|$. Then (49) can be approximated by the product

$$I(00l;\Psi)\propto(2\mu_1\cos^2\Psi+2\mu_2\sin^2\Psi)^{-1}\times\{|F_0|^2+8FA_0[C_{lz}(f'_{11}\cos^2\Psi+f'_{22}\sin^2\Psi)-S_{lz}f''_{12}\sin 2\Psi]+8FB_0[C_{lz}(f''_{11}\cos^2\Psi+f''_{22}\sin^2\Psi)-S_{lz}f'_{12}\sin 2\Psi]\}. \quad (50)$$

For a conventional data collection in bisecting geometry ($\Psi=0$), (50) reduces to

$$I(00l;0)\propto[|F_0|^2+8C_{lz}(FA_0f'_{11}+FB_0f''_{11})]/2\mu_1 \quad (51)$$

compared to $|F_0|^2/\mu$ for isotropic AS. This comparison is an instructive example of the general effect of AAS on the intensities of conventionally measured allowed reflections. Provided the diagonal elements of the 'edge' atom's **f** tensor deviate from $f'_0+if''_0$ (here by $f'_{11}+if''_{11}$) there will be an intensity contribution. The relative change of intensity can then be approximated by

$$\Delta I/I\simeq 8C_{lz}(FA_0f'_{11}+FB_0f''_{11})/|F_0|^2 \quad (52)$$

and increases therefore with decreasing reflection strength. For the second factor of (49), the difference between the intensity values $I(00l;0)$ and $I(00l;\pi/2)$ is

$$\Delta I=C_{lz}[FA_0(f'_{11}-f'_{22})+FB_0(f''_{11}-f''_{22})] \quad (53)$$

showing that sign and modulation of the AAS contribution to $I(00l;\Psi)$ can vary with increasing order of l.

The second case assumes that $|f_{11}|^2$ and $|f_{22}|^2$ are negligibly small compared to $|f_{12}|^2$. Then, $\mu_1=\mu_2=\mu_0$ and (49) reduces to

$$I(00l;0)\propto|F_0|^2/2\mu_0+16S_{lz}^2|f_{12}|^2(\sin^2\Theta_l)\times[\mu_0(1+\sin^2\Theta_l)+\mu_3\cos^2\Theta_l]^{-1} \quad (54)$$

so that the AAS contribution is always positive and the relative intensity change is approximately

$$\Delta I/I\simeq 16S_{lz}^2|f_{12}|^2(\sin^2\Theta_l)/|F_0|^2. \quad (55)$$

Again, the effect gains importance with decreasing reflection intensity, but also with increasing scattering angle. The difference between the intensity values of (49) at $\Psi=0$ and $\Psi=\pi/2$ tends to vanish, *i.e.* there will be no modulation of $I(00l;\Psi)$. The observation of a significant intensity variation with Ψ implies therefore dominance of the first case, rather than the second.

Comparing, finally, (51) and (54) shows an interesting consequence for the Bijvoet difference $X(00l)=I(00l;0)-I(00\bar{l};0)$. While (54) implies for the latter case that AAS has no effect on $X(00l)$, this is not true for the first case considered. Since $FA(00l)_0$ and $FB(00l)_0$ are different from $FA(00\bar{l})_0$ and $FB(00\bar{l})_0$, respectively (while $C_{lz}=C_{\bar{l}z}$), the corresponding differences will mix with f'_{11} and f''_{11}, and thus lead to a modified $X(00l)$. This argument can also, of course, be extended to general reflections and may therefore be taken as a warning that the determination of isotropic f''_0 from experimental Bijvoet differences may become questionable in the immediate vicinity of an absorption edge.

Experimental

The $LiHSeO_3$ sample was a large transparent synthetic crystal ($20\times30\times50$ mm) grown from aqueous solution. This crystal is depicted and described

thoroughly in the report of its physical properties (Recker, Wallrafen, Haussühl & Shao Zong Shu, 1984) to which the interested reader is referred for details. Here it suffices to say that the crystal is bound (among other faces) by a large pinacoid, {001} of 11×18 mm, and a smaller one, {010} of 4×18 mm, where the setting is chosen according to the structure determination by Chomnilpan & Liminga (1979), $a_o = 5.058$, $b_o = 11.187$, $c_o = 5.221$ Å. Thus, measurements of the serial reflections $00l$ and $0k0$ from the extended faces (001) and (010), respectively, could be easily obtained provided care was taken that the area illuminated by the primary beam of 1×1 mm cross section remained unaltered upon rotation around the scattering vector. For the smaller face, (010), this demanded a sufficiently large scattering angle at the Se K-absorption edge ($\lambda = 0.9797$ Å, 12.6545 keV) so that reflections $0k0$ with $k<7$ were not accessible.

The experiments were carried out on the two-axis diffractometer installed at beam line G3 at HASYLAB (Bonse & Fischer, 1981) during dedicated beam time (DORIS II being operated at 3.7 GeV, critical energy 9 keV, maximum injected current 100 mA). The radiation was monochromatized by an asymmetrically cut Ge(311) flat double-crystal arrangement with fixed exit ($\Delta E/E \simeq 3\times10^{-4}$). The experimental set-up and the procedure are described in detail in KPE. The only difference concerns the access of the K-absorption edge which was detected by monitoring the fluorescence yield from the large (001) face upon tuning the energy.

The crystal was mounted and oriented with [100] perpendicular to the beam axis and [001] or [010], respectively, pointing into the vertical direction for $2\Theta = 0°$ so that any Ψ setting could be read directly from the Φ circle.

Results and discussion

The proof of FRED and the ensuing location of the optimal resonance energy were performed by intensity measurements, $I(003; E)$, at $\Psi = 0°$. Fig. 4 shows the variations of both the intensity of the 'forbidden' reflection 003 and of the fluorescence yield from the (001) face upon passing across the Se K-absorption edge. The large and narrow peak of $I(003)$ occurring on the low-energy side of the spectrum must be attributed to multiple scattering (*Umweganregung*). It disappeared quickly upon changing Ψ. This peak has not been removed in order to show how multiple scattering can interfere with FRED. Measurements for sufficient numbers of Ψ settings are therefore always required for safe discrimination.

All measurements, $I(\mathbf{h}; \Psi)$, were carried out at the energy of the second broad intensity maximum (Fig. 4) at about 10 eV above the edge (where the edge position is assigned to the center of the steep increase of fluorescence).

'Forbidden' reflections

$I(\Psi)$ observations are depicted in Figs. 5 (*a*)-(*d*) for the 'forbidden' reflections 001, 003, 005 and 007. Similar results for the likewise 'forbidden' reflections 070, 090 and 0,11,0 are omitted. As described in KPE, each experimental point represents the integrated net intensity obtained from an on-line normalized ω-scan profile (61 steps, $\Delta\omega = 0.06°$, 5–10 s counting time per step). The assignment of error bars is omitted, not only for clarity but also because:

(i) errors from counting statistics alone were usually of about the size of the dots (except for very weak intensities);

(ii) errors due to energy instability (beam instability) could not be pinpointed, *i.e.* a correlation between the scatter of the intensity values and the permanently recorded vertical beam position was not detectable (it is, however, clear that energy instability is a major source of error and that measurements at a higher speed than permitted by the present experiment would be beneficial to both data quality and its assessment);

(iii) multiple scattering contributions can never be entirely excluded;

(iv) errors arising from the integration procedure (manual background assignment) may be considerable at Ψ settings for which the AAS effect is small.

Assuming totally σ-polarized radiation, fits of the model curve (45) to the observations were carried out using the program *MINUIT* (James & Roos, 1987). For this purpose, (45) was used for the cases of

(*a*) neglecting and

(*b*) including anisotropic absorption.

Overall agreement indices R, intensity values at $\Psi = 0°$ and $\Psi = 90°$ taken from the adjusted intensity functions and quotients $Q = I(\mathbf{h}; 0)/I(\mathbf{h}; \pi/2)$ are listed in Table 1. Also included are the respective quotients Q_{zij} and Q_{yij} carrying the structural

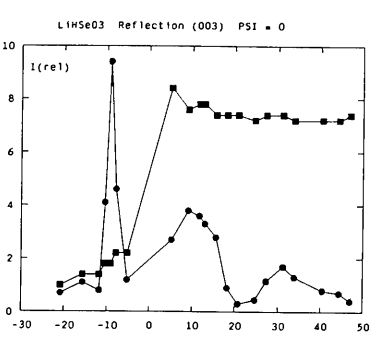

Fig. 4. Energy dependence of the 'forbidden' reflection 003 ($\Psi = 0°$) at the Se K-absorption edge (filled circles). Filled squares indicate the fluorescence yield from the (001) face.

Table 1. *Results of model fits to observed $I(\mathbf{h}; \Psi)$ values*

R: conventional overall agreement index; $I(0)$, $I(\pi/2)$: relative intensity values taken from adjusted I functions; Q: observed intensity ratio $I(0)/I(\pi/2)$; for definition of Q_{zij}, Q_{yij} see text (equation 47); IA: assuming isotropic absorption; AA: considering anisotropic absorption.

		IA				AA			
	hkl	R	$I(0)$	$I(\pi/2)$	Q	R	$I(0)$	$I(\pi/2)$	Q
	001	0.058	102.5	2.78	36.87	0.051	99.5	0.98	101.5
	003	0.097	134.2	0.794	169	0.081	140	4.82	28.96
	005	0.040	49.3	4.46	11.05	0.032	48.3	3.51	15.31
	007	0.068	27.9	3.57	7.8	0.070	28.0	3.76	7.46
	004	0.021	11.0	13.5		0.019	10.9	13.25	
	006	0.012	12.9	10.1		0.011	13.1	10.25	
Q_{z31}					4.58				0.285
Q_{z51}					0.300				0.151
Q_{z71}					0.212				0.073
Q_{z53}					0.065				0.528
Q_{z73}					0.046				0.257
Q_{z75}					0.707				0.487
	070	0.125	2.94	30.75	0.0956	0.071	0.67	25.3	0.0265
	090	0.061	3.9	8.07	0.483	0.062	3.7	7.88	0.469
	0110	0.060	2.38	4.8	0.496	0.053	2.51	5.0	0.502
Q_{y97}					5.05				17.7
$Q_{y11,7}$					5.19				18.94
$Q_{y11,9}$					1.02				1.07

information (47). Comparing the results of the fits (a) and (b), one finds similar R values but considerable numerical differences between corresponding Q and as a result between the Q_{zij} and Q_{yij} values. These differences are clearly due to the small and less-reliable intensities entering Q.

All curves of Fig. 5 as well as the R values show that the observed intensity variations of the 'forbidden' reflections can be explained satisfactorily by the developed scattering model. For case (b), the mostly lower agreement indices indicate an improved description of the Ψ dependence so that the treatment of absorption [(41)-(43)] appears justified [except for two reflections, probability estimates based on Hamilton's (1965) R test are above 95%]. As a consequence, the $I(0)$ and $I(\pi/2)$ values taken from fits (b) are considered more reliable than those from (a).

Allowed reflections

For the investigated 'forbidden' reflections (except 070), the effect of anisotropic absorption on $I(\mathbf{h}; \Psi)$ appears small. This picture remains qualitatively unaltered for the allowed reflections 004 and 006, both depicted in Fig. 6. Fits of (49) to the observed intensities yielded agreement indices $R = 0.019$ (0.021 for isotropic μ) for 004 and $R = 0.011$ (0.012) for 006 (Table 1). The two $I(\mathbf{h}; \Psi)$ distributions show not only significant variations (±10%), but moreover a reversal of sign for $\Delta I(00l) = I(00l; 0) - I(00l; \pi/2)$, *i.e.* $\Delta I(004)$ is positive, $\Delta I(006)$ negative (Table 1). In view of the discussion of (49), these different Ψ dependencies imply that $|f_{11}|^2$ and $|f_{22}|^2$ cannot be neglected compared to $|f_{12}|^2$, the second term of (49) must dominate, and (50)-(53) are applicable. Thus, Figs. 6(a) and (b) are instructive illustrations of the effect caused by mixing the real and imaginary parts, FA_0, FB_0, of the structure factor (including isotropic AS) with the AAS contributions.

Localization of the 'edge atom'

In space group $P2_12_12_1$ any four symmetry-equivalent atoms are located at z, $\frac{1}{2}-z$ and $\frac{1}{2}+z$, $-z$ (the same relations hold for x and y). Therefore, it suffices to evaluate a z indication for the Se atom within the range $0 \le z < 0.25$. For the investigated $00l$ reflections the functions Q_{zij} (calc.) [(47), $Y = 1$] were calculated for increments $\Delta z = 0.001$, and depicted in Fig. 7. These curves possess mirror symmetry with respect to $z = 0$, $\frac{1}{4}$, $\frac{1}{2}$, $\frac{3}{4}$. They vary over orders of magnitude and they become generally steeper the larger the product of the involved indices, $l_i l_j$. Towards $z = 0.0$ and $z = 0.25$ the functions flatten out upon approaching finite values. This feature implies that the derivation of a coordinate close to 0.0 or 0.25 will demand more accurate Q values (small gradients dQ_{zij}/dz) than that of intermediate values (where large gradients prevail).

Using the experimental quotients Q_{zij}(obs.) of Table 1, column AA, z(Se) indications were derived by comparison with the Q_{zij}(calc.) functions. For the present evaluation all z coordinates for which Q_{zij}(calc.) was found within the range Q_{zij}(obs.) ± 50% (±100%) for Q_{zij}(obs.) > 0.3 (≤0.3) were selected and represented by the black bars of Fig. 8(a). The result is a pattern of possible z coordinates. The z range common to all pairs of reflections was then considered significant and its center was taken as the experimental z coordinate with an uncertainty given by the range itself. Fig. 8(a) yields a unique z(obs.) = 0.2375 (125) (see combinations 5,3 and 7,5) compared

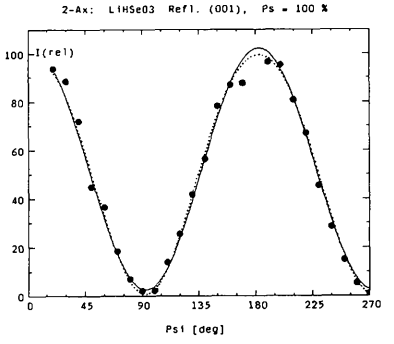

(*a*)

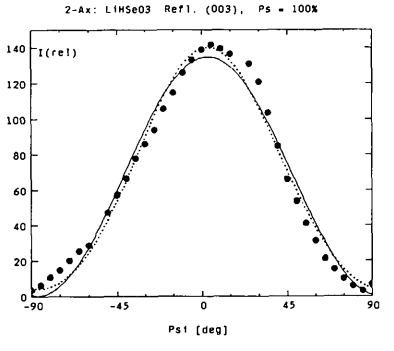

(*b*)

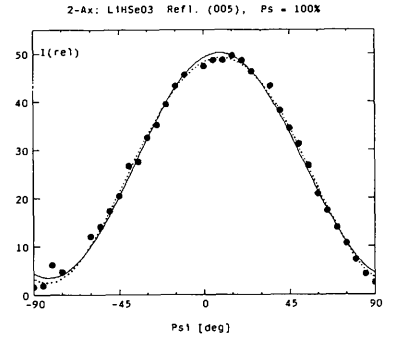

(*c*)

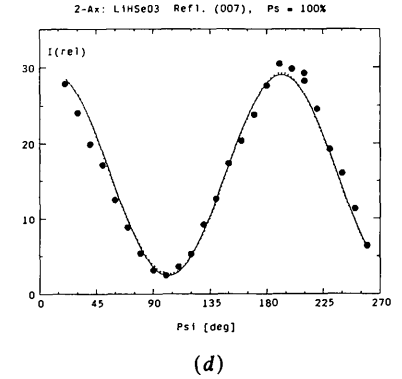

(*d*)

Fig. 5. Intensity variations upon Ψ rotation around the scattering vector and fits of model functions (assumed 100% σ-polarized radiation) for 'forbidden' 00*l* reflections. Solid line: neglecting anisotropic absorption; dotted line: including anisotropic absorption. (*a*) 001, (*b*) 003, (*c*) 005, (*d*) 007.

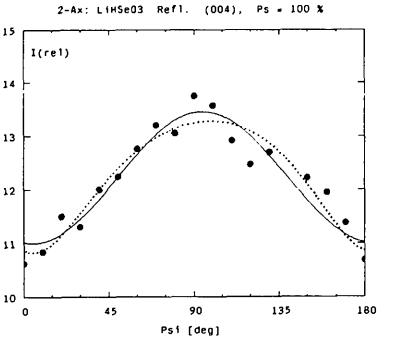

(*a*)

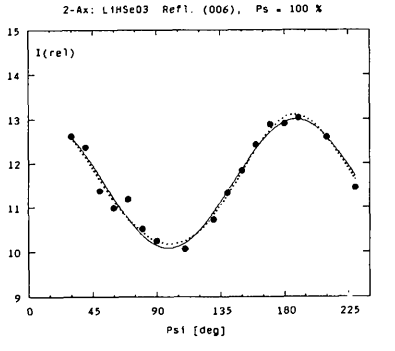

(*b*)

Fig. 6. Intensity variations of allowed 00*l* reflections. (*a*) 004, (*b*) 006. Key as Fig. 5.

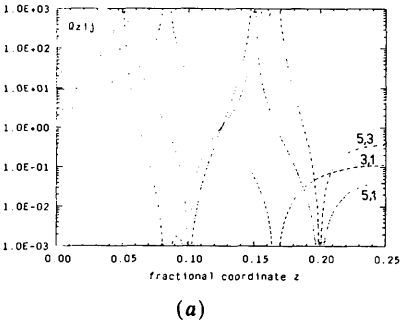

(*a*)

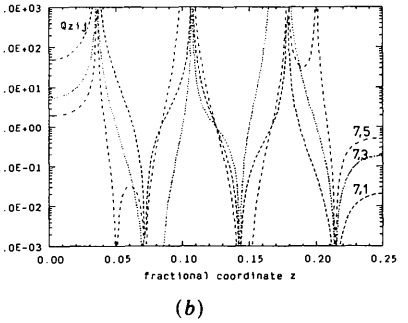

(*b*)

Fig. 7. Unique parts of the functions Q_{zij} in the range $0 \leq z < 0.25$. Reflection combinations (*a*) (3,1), (5,1), (5,3); (*b*) (7,1), (7,3), (7,5).

to the 'true' coordinate $z = 0.23316\,(4)$ (Chomnilpan & Liminga, 1979). Thus, the experimental value deviates only by $\Delta z = 0.004$ or 0.02 Å from the true one.

The present assignment of uncertainty ranges to the Q_{zij} is arbitrary and the lengths of the bars in Fig. 8(*a*) and the derived z indication and its uncertainty depend on that choice. But the assignment is not critical as other choices show. Provided the Q_{zij} uncertainties are chosen large enough to yield overlapping bars, similar z indications are obtained though with different uncertainties. The assignment of a 100% error to the small Q_{zij}(obs.) seems justified since these values are not only less reliable but also systematically overestimated in view of the π component of the incident radiation being neglected in the intensity model.

Applying the corresponding procedure to Q_{yij}(obs.) yielded the results given in Fig. 8(*b*). Compared to Fig. 8(*a*) this pattern shows much smaller ranges of indications due to the larger Q_{yij} values fitting into regions with large gradients. Here, we find two indications, y(obs.) = 0.150 (5), and another at y(obs.) = 0.200. The first compares well with the 'true' coordinate, $y = 0.14709\,(2)$ ($\Delta y = 0.0029 \hat{=} 0.032$ Å); the second is wrong. This ambiguity must be attributed to the availability of only three (0*k*0) reflections and particularly to the lack of a reflection with $k < 7$. (The allocated beam time precluded measurements on a fourth reflection, 0,13,0, which would have increased the resolution.) On the other hand, the result indicates that the method can work even under restricted conditions.

Finally, it is interesting to note that applying the described procedure to the Q_{zij} values obtained without considering anisotropic absorption (Table 1, column IA) yielded a comparable z indication [z = 0.240 (10)] only upon discarding Q_{z31} and assigning an uncertainty range of 0.0–0.6 to Q_{zij}(obs.) ≤ 0.3. Similarly, the y coordinate was found correctly upon discarding $Q_{y11,7}$, but then, of course, only from two indications. These findings present two aspects. Firstly, neglecting the absorption effects seems not necessarily fatal with respect to obtaining partial structure information from FRED. (However, insufficient data quality should be compensated for by augmenting the data basis.) Secondly, the results of the data fits are supported thus giving additional credit to the treatment of anisotropic absorption.

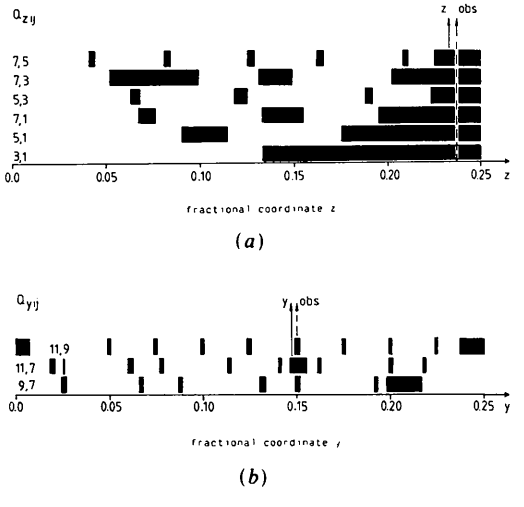

Fig. 8. Experimental fractional-coordinate indications (obs.) for the Se atom as obtained from combining $I(\mathbf{h}_i; \Psi)$ and $I(\mathbf{h}_j; \Psi)$. For details see text. (*a*) z(Se), (*b*) y(Se) (z and y indicate 'true' values).

Concluding remarks

For X-ray diffraction from a non-perfect crystal, the occurrence of AAS in the vicinity of an absorption edge requires, in principle, the simultaneous consideration of both X-ray transmission through and kinematic Bragg diffraction in the crystal. Due to AAS-induced pleochroism and birefringence the properties of the radiation arriving at a diffracting volume element dV, *i.e.* a crystallite inside the mosaic crystal, are generally different from those of the primary beam. Likewise are the properties of the radiation emerging from the crystal different from those of the radiation diffracted by the element under consideration. As a consequence, not only the polarization correction but also the absorption correction can no longer be factorized in the description of the total diffracted intensity. Instead, the intensity contribution of each volume element has to be worked out, and the subsequent integration over the crystal volume describes then the observable reflection intensity.

Both processes, transmission and diffraction in presence of AAS, have been subjects of separate studies (PKF and KPE) giving experimental evidence of the applicability of the respective models. The present contribution merges the two models into one which (apart from Lorentz and extinction corrections) describes the observations directly in terms of the crystal structure, of the isotropic (non-resonant and resonant) scattering, of the anisotropic resonant scattering (AAS) and of the properties of both radiation and crystal. Neglecting AAS restores the conventional formalism. The model is valid for totally polarized and non-polarized radiation. [General polarization can also be handled by introducing the Stoke's formalism as used by Fanchon & Hendrickson (1990).]

The intimate relation between structure factor and refractive index (optical theorem, Kramers–Kronig relation) implies that polarization-dependent diffraction and transmission effects can be highly correlated. However, the degree to which AAS can modify the transmission depends on the weight of the partial structure of the absorbing 'edge' atoms with respect

to that of the rest structure. This is because for scattering in the forward direction all atomic geometric terms are unity. Thus, for $\sum Z_{edge} \ll \sum Z_{rest}$, an anisotropy of the refractive index will be small, whereas for the opposite case anisotropy effects of transmission can be considerable. Such a distinction cannot be made for the diffraction under $2\Theta \neq 0^0$. Then, the AAS contributions mix with the structure factor (including AS) so that they generally gain importance with increasing scattering angle and/or (systematically or accidentally) decreasing reflectivity. Though this applies to all reflections, the effects of AAS become particularly evident for the space-group 'forbidden' reflections due to screw axes and/or glide planes which may be no longer systematically extinct. Since these reflections are due exclusively to the partial structure of the 'edge' atom(s), they are of special interest. Firstly, they simplify the model considerably; secondly, they consist of complete information about AAS including its spatial relation with respect to the chemical bonds; thirdly, they reflect the projection of the partial structure onto the respective crystal axes and/or zones. Thus, they may be exploited for partial structure analysis without requiring any detailed knowledge about the resonance itself. In some cases, even scaling of the FRED intensities is not required. Such a case is space group $P2_12_12_1$.

The experimental evidence collected within 7 d of beam-time allocation and reported in the second part of this paper gives direct proof of the occurrence of AAS in $LiHSeO_3$ (at the Se K-absorption edge) and of the validity of the underlying scattering model. Satisfactory agreement is obtained for the observed intensity variations upon rotation about the scattering vector of both 'forbidden' and allowed reflections. Evidence is also obtained for the correct treatment of transmission. We are, however, well aware of the fact that the experimental basis is not adequate (quantitatively rather than qualitatively) for a definite judgement. (This would require measurements on a larger number of reflections demanding an improved experimental technique, in particular higher speed.) Thus, future work is planned on a conventional diffractometer using the bathing method. This is expected to yield a larger data set (including allowed reflections) permitting a quantitative separation of diffraction and transmission effects by refinement techniques.

The experimental proof of the predicted possibility of obtaining partial structure information, here to locate the Se atom in the asymmetric unit, from only a few 'forbidden' reflections is another finding of this study. Again, a larger experimental base is needed for more experience with the practical benefits of the method. At present, it seems therefore too early for far-reaching statements. Nevertheless, the outcome is promising and suggests various applications on other compounds. One interesting case is a large organic structure with two or more different 'edge' elements, one atom of each per asymmetric unit. Knowing the different 'edge' atom positions in the molecule, one should be able to confine its orientation and location to a limited number of possibilities to be explored in combination with other methods of structure solution. Another option concerns the determination of cation distributions in known mineral structures. Model calculations for olivine, spinel and garnet show that in each case only one of the two cation positions, $M1$ and $M2$, contributes to FRED. Provided there is AAS at all, the signal will be proportional to the squared occupancy of that position by the 'edge' element under consideration. Thus, although the investigation of AAS-induced FRED will hardly become a standard technique, it is conceivable that it may be a complementary tool in the determination of complex structures.

This work has received financial support by the Bundesminister für Forschung und Technologie (AZ05 457 IX) which is gratefully acknowledged. Our thanks are also due to Dr F. Wallrafen, Universität Bonn, Germany, for providing the crystal sample, to Dr K. Eichhorn, HASYLAB/DESY, Germany, for help with the experiments, and to Professor Dr K. Fischer, Universität des Saarlandes, Germany, for many fruitful discussions.

References

BONSE, U. & FISCHER, K. (1981). *Nucl. Instrum. Methods*, **190**, 593-603.

CHOMNILPAN, S. & LIMINGA, R. (1979). *Acta Cryst.* B**35**, 3011-3013.

FANCHON, E. & HENDRICKSON, W. A. (1990). *Acta Cryst.* A**46**, 809-820.

HAMILTON, W. C. (1965). *Acta Cryst.* **18**, 502-510.

JAMES, F. & ROOS, M. (1987). *MINUIT* program. Program Library No. D506. CERN Computer Centre, Grenoble, France.

JAMES, R. W. (1982). *The Optical Principles of the Diffraction of X-rays*. Woodbridge, CT: Ox Bow Press.

JONES, R. C. (1941). *J. Opt. Soc. Am.* **31**, 488-493, 500-503.

JONES, R. C. (1948). *J. Opt. Soc. Am.* **38**, 671-685.

KIRFEL, A. & PETCOV, A. (1991). *Z. Kristallogr.* **195**, 1-15.

KIRFEL, A., PETCOV, A. & EICHHORN, K. (1991). *Acta Cryst.* A**47**, 180-195.

PETCOV, A., KIRFEL, A. & FISCHER, K. (1990). *Acta Cryst.* A**46**, 754-763.

RECKER, K., WALLRAFEN, F., HAUSSÜHL, S. & SHAO ZONG SHU (1984). *Z. Kristallogr.* **169**, 249-256.